The Astronomical Journal, 137:3900–3910, 2009 April doi:10.1088/0004-6256/137/4/3900

NEW PRECISION ORBITS OF BRIGHT DOUBLE-LINED SPECTROSCOPIC BINARIES. III. HD 82191, ω DRACONIS, AND 108 HERCULIS

Francis C. Fekel[1,3], Jocelyn Tomkin[2], and Michael H. Williamson[1]
[1] Center of Excellence in Information Systems, Tennessee State University, 3500 John A. Merritt Boulevard, Box 9501, Nashville, TN 37209, USA; fekel@evans.tsuniv.edu
[2] Astronomy Department and McDonald Observatory, University of Texas, Austin, TX 78712, USA; jt@alexis.as.utexas.edu
Received 2008 December 9; accepted 2009 January 20; published 2009 March 6

ABSTRACT

We have determined improved spectroscopic orbits for three double-lined binaries, HD 82191 (Am), ω Dra (F5 V), and 108 Her (Am), using radial velocities from the 2.1 m telescope at McDonald Observatory, the coudé feed telescope at Kitt Peak National Observatory, and 2 m telescope at Fairborn Observatory. The orbital periods range from 5.28 to 9.01 days, and all three systems have circular orbits. The new orbital dimensions ($a_1 \sin i$ and $a_2 \sin i$) and minimum masses ($m_1 \sin^3 i$ and $m_2 \sin^3 i$) have accuracies of 0.2% or better. Our improved results confirm the large minimum masses of HD 82191 and also agree with the values previously found for ω Dra. However, for the components of 108 Her our minimum masses are about 20% larger than the previous best values. We conclude that both components of HD 82191 as well as the primary of 108 Her are Am stars. However, the A9 secondary of 108 Her has normal abundances. We estimate spectral types of F4 dwarf and G0 dwarf for the components of ω Dra. The primaries of the three binaries are synchronously rotating as is the secondary of 108 Her. The secondaries of HD 82191 and ω Dra are possibly synchronously rotating.

Key words: binaries: spectroscopic – stars: individual (HD 82191, omega Dra, 108 Her)

1. INTRODUCTION

Direct determination of stellar masses is possible for binary stars that are resolved as both a spectroscopic and visual binary, enabling three-dimensional orbits to be determined. In addition to the individual masses of the stars, such a combined orbit results in an "orbital parallax" of the system, producing a precise distance. Over the past several decades, advances in ground-based optical and near-infrared interferometry have increased the overlap of spectroscopic and visual binary domains (Quirrenbach 2001). Recent work on individual systems (e.g., Hummel et al. 2001; Boden et al. 2006) has led to important comparisons with evolutionary theory.

An ever increasing number of orbits, mostly for newly identified systems, are listed in SB9, the Web-based spectroscopic binary orbit catalog (Pourbaix et al. 2004). However, many of the older spectroscopic orbits in that database date from the era of photographic plates, and so, would limit the precision of three-dimensional orbits. To partially remedy that situation, in this series of papers (Tomkin & Fekel 2006, 2008) we report the determination of improved spectroscopic orbits for bright field spectroscopic binaries, which are the most accessible systems to interferometry. Such revised spectroscopic orbits will complement prospective interferometric observations. The three stars, HD 82191, ω Dra, and 108 Her, that are analyzed in this paper have been grouped together because unlike the six systems previously discussed in this series, we have adopted circular orbits for them. Table 1 provides basic data for the three systems.

[3] Visiting Astronomer, Kitt Peak National Observatory, National Optical Astronomy Observatory, operated by the Association of Universities for Research in Astronomy, Inc. under cooperative agreement with the National Science Foundation.

2. BRIEF HISTORY

2.1. HD 82191 = HIP 46704

Young (1942) reported the discovery of the duplicity of HD 82191 [$\alpha = 09^h31^m17^s.39$, $\delta = 27°23'14''.1$ (2000)]. He remarked that its spectrum is undoubtedly double lined although it was barely resolved on the 66 Å mm^{-1} photographic plates that were obtained at the David Dunlap Observatory (DDO). The combined spectral class was estimated as being A0. Six follow-up spectra were obtained between 1946 and 1948. However, over two decades would pass before an extended observational effort at DDO by Heard & Hurkens (1973) resulted in 43 additional spectrograms and an analysis of the star system. They computed an orbital period of 9.0119 days and determined that the orbit is essentially circular. Comparing the line ratios of the iron lines of the sharp-lined components, they concluded that since the Fe II lines of the two components are more equal in intensity than the Fe I lines, the secondary star has the earlier spectral type. Their derived minimum masses for the components are so large, $\sim$2 $M_\odot$, that Heard & Hurkens (1973) suggested that the system is eclipsing. Based on the orbital prediction, Fernie (1974) detected a primary eclipse that lasted approximately 3 hr. However, because he observed a V mag depth of only 0.03, Fernie (1974) suggested that the eclipse should be verified. Gulliver (1971) noted that HD 82191 is an Am star. Abt (2004) did not confirm the Am spectral classification, but instead gave a combined spectral type of A0 Vs.

2.2. ω Dra = HR 6596 = HD 160922

The naked eye star ω Dra [$\alpha = 17^h36^m57^s.09$, $\delta = 68°45'28''.7$ (2000)] was first observed spectroscopically at the very end of the 19th century. From four radial velocities obtained at Lick Observatory, Campbell (1899) announced that ω Dra was a single-lined spectroscopic binary with rapid variability.

However, it was not until seven years later that an extensive series of plates was acquired at that observatory, enabling Turner (1907) to determine orbital elements from 26 observations. He characterized the star as F-type with rather broad, fuzzy lines and found an orbital period of 5.27968 days and an eccentricity very close to zero. Both Luyten (1936) and Lucy & Sweeney (1971) reexamined the orbital velocities used by Turner (1907) and adopted a circular orbit. As part of a survey of spectroscopic binaries among F- and G-type dwarfs and subgiants, Abt & Levy (1976) reobserved ω Dra at Kitt Peak National Observatory (KPNO) and were the first to detect lines of the secondary. They noted that a faint visual companion, which is over 70″ away, seems to have a common proper motion with the brighter system. In a survey for additional companions to 25 known binary systems, at Haute-Provence Observatory (HPO) Mayor & Mazeh (1987) obtained a third set of radial velocities for ω Dra. The center-of-mass velocities derived for the three data sets are quite similar, indicating no close companion to the binary.

Both Roman (1950) and Slettebak (1955) classified the combined spectrum of ω Dra as F5 V, similar to the more recent spectral type of F4 V given by Cowley (1976). Herbig & Spalding (1955) estimated a projected rotational velocity of <20: km s^{-1}, while Slettebak (1955) found a value of <25 km s^{-1}, and Levato (1975) determined 13 km s^{-1}. Favata et al. (1995) measured $v \sin i$ values of $\leqslant$14 km s^{-1} for both components.

2.3. 108 Her = HR 6876 = HD 168913

The star 108 Her [$\alpha = 18^{\rm h}20^{\rm m}56\overset{\rm s}{.}97$, $\delta = 29^\circ 51' 32\overset{''}{.}1$ (2000)] was discovered to be a binary early in the twentieth century. From plates taken at Mount Wilson Observatory in 1911, Adams (1912) listed four radial velocities that showed a significant variation. Using velocities from 17 plates acquired at the Astrophysical Observatory, Potsdam, Ludendorff (1914) determined a circular orbit with a period of 5.1460 days and found evidence of lines of the secondary. Shortly thereafter, Daniel & Jenkins (1916) made a much more extensive analysis with 93 spectrograms that were obtained at Allegheny Observatory from 1912 through 1914. While they reported that lines of the primary were fairly easy to measure, they stated that lines of the secondary were faint and hard to measure. Nevertheless, they were able to determine velocities of the secondary from the majority of their spectrograms. Nearly 70 years later Abt & Levy (1985) obtained 22 new observations at KPNO. They concluded that their velocities provided a small improvement in the period and produced an essentially circular orbit. While such properties of the orbit were in agreement with the results of Daniel & Jenkins (1916), Abt & Levy (1985) found a substantially smaller semiamplitude velocity for the secondary that resulted in a mass ratio of 1.11.

Cowley et al. (1969) classified 108 Her as A5m: or a mild metallic-lined star, where their subclass is a measure of the Ca K line. Bidelman (Abt & Bidelman 1969), however, called it a definite Am star. Bertaud (1970) found A5 for the Ca K line, and F0 for the metallic spectrum. More recently, Abt & Morrell (1995) also noted that the composite spectrum was that of an Am star, classifying it as A3/F0/F0 for the Ca K, Balmer, and metal lines, respectively.

Stickland (1973) determined abundances for the components of 108 Her, confirming the enhancement of iron in both components. However, only the primary exhibited a deficiency of calcium. Burkhart & Coupry (1991) also examined the calcium and iron abundances of the components of 108 Her, confirming that the primary is an Am star, but they concluded that the secondary has normal abundances of those two elements. Both components are slowly rotating, with $v \sin i \leqslant 20$ km s^{-1} (Abt 1975).

3. OBSERVATIONS AND RADIAL VELOCITIES

From 2002 through 2006 we acquired observations at McDonald Observatory with the 2.1 m telescope, the Sandiford Cassegrain echelle spectrograph (McCarthy et al. 1993), and a Reticon CCD. The spectrograms cover the wavelength range 5700–7000 Å and have a resolving power of 49,000. From 2004 through 2008 we also obtained observations at KPNO with the coudé feed telescope and coudé spectrograph. Nearly all were made with a TI CCD detector, and those spectrograms were centered at 6430 Å, cover a wavelength range of 84 Å, and have a resolution of 0.21 Å or a resolving power of just over 30,000. The TI CCD was unavailable in 2008 September, and so a Tektronics CCD, designated T1KA, was used instead. With that CCD the spectrum was centered at 6400 Å, the wavelength range was increased to 172 Å, but the resolution was reduced to 19,000. Further details about our observations and data reduction are given in Tomkin & Fekel (2006).

For one of the three stars, ω Dra, we have obtained a significant number of additional observations, beginning in 2004, with the Tennessee State University 2 m automatic spectroscopic telescope (AST), a fiber-fed echelle spectrograph, and a 2048 × 4096 SITe ST-002A CCD. The echelle spectrograms have 21 orders that cover the wavelength range 4920–7100 Å with an average resolution of 0.17 Å. The typical signal-to-noise ratio of these observations is ~30. Eaton & Williamson (2004, 2007) have given a more extensive description of the telescope and spectrograph, operated at Fairborn Observatory near Washington Camp in the Patagonia Mountains of southeastern Arizona.

The spectra of the three systems are double lined and, at most orbital phases, the secondary lines are well separated from their primary counterparts. The procedures used to measure the McDonald and KPNO radial velocities have been described in Tomkin & Fekel (2006). Here we recall that the McDonald velocities are absolute velocities, which were set on a secure rest scale by means of the telluric O_2 and H_2O lines embedded in the stellar spectra. The KPNO velocities were determined by cross-correlation with respect to IAU radial velocity standard stars of the same or similar spectral type as the program stars. The velocities adopted for those standards are from Scarfe et al. (1990). Because a comparison of the McDonald and KPNO velocities by Tomkin & Fekel (2006) showed that they are consistent with each other to within 0.1–0.2 km s^{-1}, or better, Tomkin & Fekel (2006) decided not to adjust either set of velocities, and we have likewise not made any adjustment here.

For the Fairborn Observatory AST spectra, lines in approximately 170 regions, centered on the rest wavelengths (Moore et al. 1966) of relatively strong, mostly Fe I lines that were not extensively blended with other nearby strong features, were measured. Lines at the ends of each echelle order were excluded because of their lower signal-to-noise ratios. The wavelength scale of each spectrum was initially determined from Th-Ar comparison spectra obtained at the beginning and end of the night, and that scale was refined with the use of the telluric O_2 lines near 6900 Å, which are in each stellar spectrum. A Gaussian function was fitted to the profile of each component. If lines of the two components were blended, a double Gaussian was used to fit the combined profile. The difference between the observed wavelength, determined from the Gaussian fit, and

that given in the solar line list of Moore et al. (1966) was used to compute the radial velocity, and a heliocentric correction was applied. From the individual lines a mean velocity for each component was determined. Our unpublished velocities of several IAU standard solar-type stars indicate that the Fairborn Observatory velocities have a small zero-point offset of -0.3 km s^{-1} relative to the velocities of Scarfe et al. (1990).

4. DETERMINATION OF ORBITS AND RESULTS

We have determined the orbital elements with several computer programs. Preliminary orbits were computed with the program BISP (Wolfe et al. 1967), which implements a slightly modified version of the Wilsing–Russell method. Eccentric orbits were then determined with SB1 (Barker et al. 1967), a program that uses differential corrections. Finally, circular orbits were determined with SB1C and SB2C (D. Barlow 1998, private communication), which also use differential corrections to compute improved orbital elements. For a circular orbit the element T, a time of periastron passage, is undefined. Thus, as recommended by Batten et al. (1989), T_0, a time of maximum velocity for the primary, is used instead.

As noted in Section 3, the spectra that we obtained at three different observatories have different wavelength ranges, and thus different numbers of lines were available for measurement. In addition, the primary and secondary lines are of different qualities because the components differ in strength and, to a lesser extent, in width. Thus, the velocity precision of each set of data will vary from observatory to observatory, and the precision will also usually differ for each primary and secondary component. To determine the weight for each set of velocities, whether our own or in the literature, we computed the variances of the individual orbital solutions, which are inversely proportional to our adopted weights.

4.1. HD 82191

The 18 radial velocities of the primary that we obtained from the McDonald Observatory spectra are the most precise, and so we have used them to compute both eccentric and circular orbits. The eccentric solution produces $e = 0.0028 \pm 0.0008$, and taken at face value, the tests of Lucy & Sweeney (1971) indicate that the eccentric solution should be adopted. However, the eccentricity is extremely small and may have resulted from observational errors. In addition, the distribution of the velocities is not as uniform as one would like. In fact, only five of the 18 velocities are on the descending branch of the velocity curve. Thus, we have chosen to adopt a circular orbit solution for HD 82191.

In addition to using our new velocities from McDonald Observatory and KPNO, we have also investigated the possibility of combining those observations with the earlier photographic ones from DDO. For the primary we made individual circular orbit solutions, which resulted in weights of 1.0, 0.1, and 0.005 for the McDonald, KPNO, and DDO velocities. Then a combined solution of the McDonald and KPNO primary velocities, appropriately weighted, was computed and compared with a solution containing velocities from all three observatories. In the latter solution the inclusion of the DDO velocities extensively extends the time baseline, but the only orbital element with an improved uncertainty is the period. However, the period in the three-observatory solution changed by less than 1σ, and so we have chosen not to include the DDO velocities in our analysis. A final circular orbit solution included the velocities of the secondary, for which we assigned weights of 0.5 and 0.07 for the McDonald and KPNO velocities, respectively. The large difference between these two weights, as well as those for the primary component, 1.0 versus 0.1, reflects the fact that for HD 82191 the spectral types of its two components are significantly earlier than most of the other stars that we are observing in this program. This puts the KPNO velocities at a disadvantage, in part because of the very limited 84 Å wavelength range that we observe but also because the Fe I lines in the 6430 Å region, which are generally measured in the later-type stars, are very weak in strength, and the small number of Fe II lines in this region are also not particularly strong. The 18 McDonald Observatory and 12 KPNO observations used for this orbital solution are given in Table 2.

Table 1
Basic Properties of the Program Stars

Name	HR	HD	Spectral Type	V^a	$B-V^a$	Parallax[a] (mas)	Period (days)
...	...	82191	Am	6.64	0.080	7.11	9.01
ω Dra	6596	160922	F5 V	4.77	0.430	42.62	5.28
108 Her	6876	168913	Am	5.61	0.231	17.36	5.51

Note. [a]Perryman et al. (1997).

Table 3 lists the resulting elements for our final circular orbit, as well as the elements of Heard & Hurkens (1973). Figure 1 compares our new primary and secondary velocities with the calculated velocity curves, and zero phase is a time of maximum velocity for the primary. Inspection of Table 3 shows that our new orbital elements are generally consistent with those of Heard & Hurkens (1973) but are much more precise.

4.2. ω Dra

To determine whether an eccentric or circular orbit is more appropriate for ω Dra, we have examined the 58 Fairborn Observatory observations of the primary, which are our most precise velocities. The eccentric solution results in $e = 0.0027 \pm 0.0008$. Compared with a circular orbit solution of the same data, the tests of Lucy & Sweeney (1971) indicate that the eccentric solution should be adopted. However, once again, the eccentricity is extremely small and may simply result from observational errors. Thus, we also computed circular and eccentric solutions using the Fairborn observations of the secondary. For that eccentric solution we find $e = 0.0009 \pm 0.0009$, an even smaller value than that for the solution of the primary. In this case the tests of Lucy & Sweeney (1971) indicate that the circular orbit should be adopted, a conclusion opposite to that found for the primary. Help in resolving this apparent contradiction is provided by the ω values of the two eccentric solutions. The difference for the two components is only 2°, compared to the expected value of 180°, if the orbit were truly eccentric. Because of this result and the very small eccentricities found for both components, we have chosen to adopt a circular orbit for ω Dra.

In addition to the large number of spectrograms from Fairborn Observatory, we also obtained 21 observations at KPNO and three at McDonald Observatory, one of which was acquired at single-lined phase. Because of their small number, we have chosen to treat the McDonald observations as if they are part of the data obtained at KPNO. Another set of velocities, those of HPO (Mayor & Mazeh 1987), were also considered for possible inclusion in the final orbital solution. Thus, we computed individual orbital solutions to determine the weights for the various sets of velocities. For the primary component those weights are 1.0, 0.8, and 0.04 for the Fairborn, KPNO/

Table 2
Radial Velocities of HD 82191

Hel. Julian Date (HJD − 2,400,000)	Phase	V_1 (km s^{-1})	$(O-C)_1$ (km s^{-1})	Wt_1	V_2 (km s^{-1})	$(O-C)_2$ (km s^{-1})	Wt_2	Source[a]
52,608.971	0.351	−31.2	−0.3	1.0	62.7	0.1	0.5	McD
52,609.978	0.462	−58.7	0.0	1.0	95.4	0.1	0.5	McD
52,719.710	0.639	−34.7	0.2	1.0	67.3	0.0	0.5	McD
52,719.864	0.656	−28.8	−0.1	1.0	59.9	0.0	0.5	McD
52,749.636	0.959	82.4	0.1	1.0	−71.3	−0.3	0.5	McD
52,750.658	0.073	77.4	0.2	1.0	−65.0	0.0	0.5	McD
53,042.926	0.504	−60.6	0.1	1.0	97.5	−0.2	0.5	McD
53,043.758	0.596	−47.8	0.1	1.0	82.5	−0.1	0.5	McD
53,044.847	0.717	−3.2	−0.1	1.0	30.0	0.3	0.5	McD
53,074.702	0.030	83.5	0.1	1.0	−72.0	0.3	0.5	McD
53,075.780	0.149	54.9	−0.1	1.0	−38.3	0.4	0.5	McD
53,108.693	0.801	34.9	−0.2	1.0	−15.1	0.1	0.5	McD
53,108.782	0.811	39.2	−0.1	1.0	−20.6	−0.4	0.5	McD
53,109.615	0.904	71.6	−0.2	1.0	−58.6	0.0	0.5	McD
53,109.768	0.921	75.9	0.1	1.0	−63.3	0.0	0.5	McD
53,121.665	0.241	9.6	−6.6	0.0	9.6	2.6	0.0	KPNO
53,123.742	0.471	−59.6	−0.1	0.1	96.8	0.5	0.07	KPNO
53,487.638	0.850	54.5	−0.4	1.0	−38.5	0.1	0.5	McD
53,488.697	0.968	83.3	0.1	1.0	−72.1	−0.1	0.5	McD
53,492.694	0.411	−49.9	−0.1	0.1	84.5	−0.3	0.07	KPNO
53,775.801	0.826	45.4	0.0	1.0	−27.2	0.2	0.5	McD
53,854.679	0.579	−52.2	−0.2	0.1	88.5	1.0	0.07	KPNO
53,855.699	0.692	−13.2	0.8	0.1	43.3	0.6	0.07	KPNO
54,222.696	0.415	−50.9	−0.3	0.1	86.3	0.5	0.07	KPNO
54,223.683	0.525	−59.2	0.6	0.1	97.4	0.7	0.07	KPNO
54,265.641	0.180	42.3	−0.5	0.1	−24.1	0.3	0.07	KPNO
54,266.638	0.291	−7.1	−0.6	0.1	33.5	−0.3	0.07	KPNO
54,526.765	0.156	52.5	−0.1	0.1	−35.4	0.6	0.07	KPNO
54,582.686	0.361	−34.5	0.1	0.1	67.3	0.4	0.07	KPNO
54,586.677	0.804	36.4	0.4	0.1	−16.8	−0.5	0.07	KPNO

Note. [a]McD: McDonald Observatory, KPNO: Kitt Peak National Observatory.

Table 3
Orbital Elements and Related Parameters of HD 82191

Parameter	Heard & Hurkens (1973)	This Study
P (days)	9.0119 ± 0.0002(est.)	9.011978 ± 0.000016
T (JD)	2,441,736.8 ± 0.7	...
T_0 (HJD)	...	2,453,128.5067 ± 0.0008
e	0.008 ± 0.005	0.00 (adopted)
ω_1 (deg)	338 ± 28	...
K_1 (km s^{-1})	72.3 ± 0.5	72.690 ± 0.048
K_2 (km s^{-1})	86.6 ± 0.5	85.750 ± 0.067
γ (km s^{-1})	10.7 ± 0.2	11.980 ± 0.029
$m_1 \sin^3 i$ ($M_\odot$)	2.04 ± 0.04	2.0146 ± 0.0035
$m_2 \sin^3 i$ ($M_\odot$)	1.70 ± 0.04	1.7078 ± 0.0026
$a_1 \sin i$ (10^6 km)	8.95 ± 0.06	9.0081 ± 0.0059
$a_2 \sin i$ (10^6 km)	10.73 ± 0.06	10.6264 ± 0.0082
rms residual (km s^{-1}) (unit weight)	...	0.15

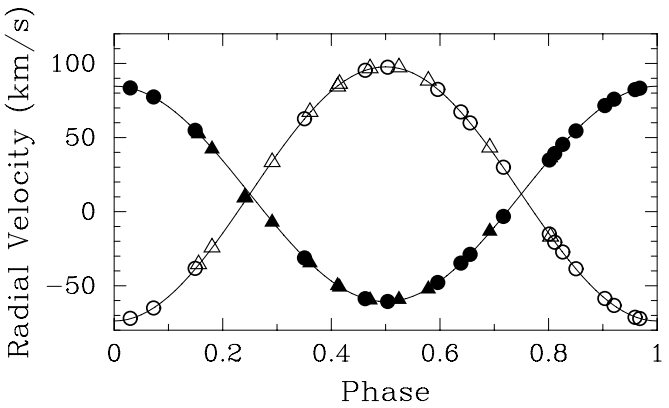

Figure 1. Radial velocities of HD 82191 compared with the computed velocity curves. The filled and open symbols represent the primary and secondary, respectively. Circles: McDonald Observatory; triangles: KPNO. Zero phase is a time of maximum velocity of the primary.

McDonald, and the HPO velocities of Mayor & Mazeh (1987), respectively. A combined solution with those three data sets, compared to a solution with just our Fairborn and KPNO/McDonald velocities, resulted in a slightly more precise period because of the longer time span of the data. However, the periods that were determined in the two solutions differ by less than their 1σ uncertainties, and the uncertainties of the other elements were not significantly improved with the addition of the Mayor & Mazeh (1987) HPO velocities. Thus, we have chosen not to include any of the HPO velocities in our later solutions.

We next determined weights for the secondary component, which are 0.6 and 0.3 for our Fairborn and KPNO/McDonald velocities, respectively. With the velocities for both stars appropriately weighted, we computed a final combined circular orbit solution. The Fairborn and KPNO/McDonald Observatory observations used for this orbital solution are given in Table 4. Table 5 lists our orbital elements and those of Mayor & Mazeh (1987). Their period, which has a slightly better uncertainty than ours, was determined by combining their elements with the T_0

Table 4
Radial Velocities of ω Dra

Hel. Julian Date (HJD − 2,400,000)	Phase	V_1 (km s^{-1})	$(O-C)_1$ (km s^{-1})	Wt_1	V_2 (km s^{-1})	$(O-C)_2$ (km s^{-1})	Wt_2	Source[a]
53,171.810	0.898	15.1	0.0	0.8	−49.8	0.0	0.3	KPNO
53,172.870	0.099	15.9	0.3	0.8	−49.7	0.7	0.3	KPNO
53,260.722	0.738	−14.7	2.1	0.0	−14.7	−4.2	0.0	McD
53,273.627	0.182	1.2	0.1	0.8	−31.4	1.1	0.3	KPNO
53,275.636	0.562	−47.3	0.2	0.8	27.3	0.0	0.3	KPNO
53,277.697	0.953	20.6	−0.2	1.0	−56.9	−0.2	0.6	Fair
53,433.922	0.542	−49.0	0.0	1.0	29.3	0.1	0.6	Fair
53,446.978	0.015	22.1	−0.1	1.0	−58.4	0.1	0.6	Fair
53,466.008	0.619	−40.6	0.0	1.0	19.0	0.2	0.6	Fair
53,468.791	0.146	7.8	−0.3	1.0	−41.2	−0.1	0.6	Fair
53,483.822	0.993	22.3	0.0	1.0	−58.2	0.4	0.6	Fair
53,487.931	0.771	−8.9	0.2	0.8	−19.7	0.2	0.3	McD
53,488.939	0.962	21.4	0.1	0.8	−57.3	0.1	0.3	McD
53,490.893	0.332	−31.6	0.3	0.8	7.9	−0.2	0.3	KPNO
53,491.885	0.520	−50.0	0.0	0.8	30.4	0.0	0.3	KPNO
53,499.964	0.050	20.6	0.1	1.0	−56.3	0.2	0.6	Fair
53,512.790	0.480	−49.9	0.1	1.0	30.6	0.2	0.6	Fair
53,526.641	0.103	14.8	−0.2	1.0	−49.6	0.0	0.6	Fair
53,530.855	0.901	15.3	−0.3	1.0	−50.4	−0.1	0.6	Fair
53,533.798	0.459	−49.3	−0.2	0.8	28.8	−0.4	0.3	KPNO
53,534.798	0.648	−36.1	−0.4	0.8	12.7	−0.1	0.3	KPNO
53,536.808	0.029	21.8	0.0	0.8	−57.6	0.4	0.3	KPNO
53,547.829	0.116	13.0	−0.1	1.0	−47.4	−0.1	0.6	Fair
53,551.968	0.900	15.0	−0.4	1.0	−50.2	−0.1	0.6	Fair
53,563.942	0.168	3.7	−0.3	1.0	−36.1	−0.1	0.6	Fair
53,564.889	0.347	−35.3	−0.5	1.0	11.2	−0.5	0.6	Fair
53,610.631	0.011	22.4	0.1	1.0	−58.6	0.0	0.6	Fair
53,626.676	0.050	20.5	−0.1	1.0	−56.4	0.1	0.6	Fair
53,630.803	0.831	3.9	0.1	1.0	−36.1	−0.3	0.6	Fair
53,639.710	0.518	−50.0	0.1	1.0	30.7	0.3	0.6	Fair
53,643.735	0.281	−21.0	−0.1	1.0	−6.0	−0.6	0.6	Fair
53,657.644	0.915	17.0	−0.3	1.0	−52.5	0.0	0.6	Fair
53,670.690	0.386	−41.5	−0.1	1.0	19.9	0.2	0.6	Fair
53,671.784	0.593	−44.4	−0.2	1.0	23.5	0.2	0.6	Fair
53,675.821	0.358	−37.0	−0.3	1.0	14.7	0.7	0.6	Fair
53,688.652	0.788	−5.6	−0.2	1.0	−24.4	0.2	0.6	Fair
53,691.709	0.367	−38.5	−0.2	1.0	16.3	0.3	0.6	Fair
53,725.645	0.795	−4.0	−0.1	1.0	−26.0	0.3	0.6	Fair
53,740.663	0.639	−37.1	0.2	1.0	15.1	0.4	0.6	Fair
53,754.035	0.172	3.1	−0.1	1.0	−35.1	0.0	0.6	Fair
53,768.987	0.004	22.4	0.1	1.0	−58.7	0.0	0.6	Fair
53,798.877	0.665	−32.5	0.0	1.0	8.9	0.1	0.6	Fair
53,813.842	0.499	−50.5	−0.2	1.0	30.9	0.2	0.6	Fair
53,836.787	0.845	6.2	−0.2	1.0	−39.1	0.0	0.6	Fair
53,849.837	0.317	−28.9	−0.2	1.0	4.4	0.2	0.6	Fair
53,852.895	0.896	14.7	−0.1	0.0	−49.4	0.0	0.3	KPNO
53,855.894	0.464	−49.3	0.1	0.0	29.5	−0.1	0.3	KPNO
53,856.778	0.631	−38.9	−0.3	1.0	16.5	0.1	0.6	Fair
53,865.779	0.336	−32.8	−0.1	1.0	9.3	0.3	0.6	Fair
53,869.742	0.087	17.2	0.1	1.0	−51.9	0.3	0.6	Fair
53,879.971	0.024	22.2	0.3	1.0	−58.1	0.1	0.6	Fair
53,882.979	0.594	−44.2	0.0	1.0	23.6	0.4	0.6	Fair
53,895.962	0.053	20.7	0.3	1.0	−56.1	0.1	0.6	Fair
53,903.957	0.567	−47.2	−0.1	1.0	26.7	−0.1	0.6	Fair
53,922.847	0.145	8.2	−0.1	1.0	−41.3	0.1	0.6	Fair
53,938.872	0.180	1.3	−0.2	1.0	−33.1	−0.1	0.6	Fair
53,996.707	0.134	10.2	0.0	1.0	−43.8	0.0	0.6	Fair
54,000.823	0.913	17.0	−0.1	1.0	−51.9	0.3	0.6	Fair
54,001.627	0.066	19.6	0.3	0.0	−54.3	0.6	0.3	KPNO
54,006.633	0.014	22.4	0.2	0.0	−58.1	0.4	0.3	KPNO
54,013.642	0.341	−33.9	−0.2	1.0	10.4	0.1	0.6	Fair
54,016.668	0.915	17.1	−0.1	1.0	−52.2	0.2	0.6	Fair
54,029.736	0.390	−42.2	−0.3	1.0	20.4	0.0	0.6	Fair
54,057.668	0.680	−29.6	−0.2	1.0	5.5	0.4	0.6	Fair

Table 4
(Continued)

Hel. Julian Date (HJD − 2,400,000)	Phase	V_1 (km s^{-1})	$(O-C)_1$ (km s^{-1})	Wt_1	V_2 (km s^{-1})	$(O-C)_2$ (km s^{-1})	Wt_2	Source[a]
54,074.729	0.911	16.6	−0.3	1.0	−52.1	−0.2	0.6	Fair
54,093.622	0.490	−50.3	−0.1	1.0	30.6	0.0	0.6	Fair
54,110.025	0.596	−43.6	0.2	1.0	22.6	−0.2	0.6	Fair
54,126.891	0.791	−4.6	0.2	1.0	−25.1	0.2	0.6	Fair
54,220.930	0.602	−43.1	0.0	0.8	21.9	0.0	0.3	KPNO
54,221.940	0.793	−4.8	−0.6	0.8	−26.1	−0.1	0.3	KPNO
54,269.793	0.857	8.5	−0.1	0.8	−42.3	−0.6	0.3	KPNO
54,367.621	0.385	−41.0	0.3	0.8	20.1	0.5	0.3	KPNO
54,584.012	0.370	−38.6	0.2	0.8	16.9	0.3	0.3	KPNO
54,586.834	0.904	16.2	0.2	0.8	−50.8	0.1	0.3	KPNO
54,729.701	0.964	21.5	0.1	0.8	−57.0	0.5	0.3	KPNO
54,732.638	0.520	−49.9	0.1	0.8	29.7	−0.7	0.3	KPNO
54,768.729	0.355	−36.4	−0.1	1.0	13.5	0.0	0.6	Fair
54,771.709	0.920	18.0	0.2	1.0	−53.2	−0.1	0.6	Fair
54,783.591	0.170	3.2	−0.3	1.0	−35.4	0.0	0.6	Fair
54,785.594	0.550	−48.5	0.0	1.0	28.8	0.2	0.6	Fair
54,790.596	0.497	−50.3	0.0	1.0	30.8	0.1	0.6	Fair
54,791.596	0.687	−28.1	0.0	1.0	3.5	0.1	0.6	Fair

Note. [a] McD: McDonald Observatory, KPNO: Kitt Peak National Observatory, Fair: Fairborn Observatory.

Table 5
Orbital Elements and Related Parameters of ω Dra

Parameter	Mayor & Mazeh (1987)	This Study
P (days)	5.279799 ± 0.000003[a]	5.2798088 ± 0.0000083
T_0 (HJD)	2,444,698.273 ± 0.005	2,453,980.1606 ± 0.0006
e	0.0 (adopted)	0.0 (adopted)
ω (deg)	...	...
K_1 (km s^{-1})	35.8 ± 0.3	36.326 ± 0.029
K_2 (km s^{-1})	45.2 ± 0.3	44.699 ± 0.039
γ (km s^{-1})	−14.1 ± 0.2	−13.975 ± 0.018
$m_1 \sin^3 i$ ($M_\odot$)	0.163 ± 0.003[b]	0.16090 ± 0.00032
$m_2 \sin^3 i$ ($M_\odot$)	0.129 ± 0.002[b]	0.13076 ± 0.00024
$a_1 \sin i$ (10^6 km)	2.60 ± 0.2	2.6373 ± 0.0021
$a_2 \sin i$ (10^6 km)	3.28 ± 0.2	3.2453 ± 0.0029
rms residual (km s^{-1}) (unit weight)	...	0.19

Note. [a] The value of the period was derived by combining the authors' elements with T_0 of Luyten (1936), based on the velocities of Turner (1907).
[b]The minimum mass values are computed in the SB9 catalog (Pourbaix et al. 2004).

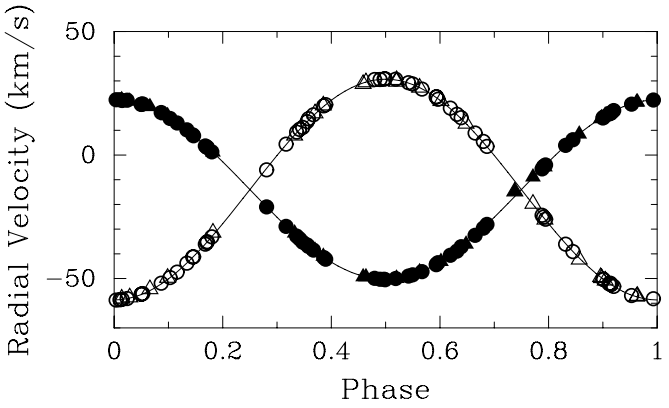

Figure 2. Radial velocities of ω Dra compared with the computed velocity curves. The filled and open circles represent the primary and secondary, respectively. Circles: Fairborn Observatory; triangles: KPNO/McDonald Observatory. Zero phase is a time of maximum velocity of the primary.

value of Luyten (1936), who based that result on an orbital solution of the radial velocities of Turner (1907). The elements of the two solutions are generally consistent but our resulting minimum masses are much more precise. Figure 2 compares our primary and secondary velocities with the calculated velocity curves. Zero phase for that orbit is a time of maximum velocity for the primary.

4.3. 108 Her

For 108 Her the 14 radial velocities of the primary that we obtained from the McDonald Observatory spectra are the most precise, and so we have used them to compute both eccentric and circular orbits. The eccentric solution produces $e = 0.0016 \pm 0.0005$, and taken at face value, the tests of Lucy & Sweeney (1971) indicate that the eccentric solution should be adopted. However, the eccentricity is extremely small, and just as in the case of HD 82191, the distribution of the velocities is not as uniform as one would like. In fact, only five of the 14 velocities are on the ascending branch of the velocity curve. Because we have almost twice as many KPNO velocities, we also computed an eccentric solution of the primary with those velocities. That solution gave an even smaller eccentricity, $e = 0.0008 \pm 0.0009$, than with the McDonald velocities. In this case, the precepts of Lucy & Sweeney (1971) indicate that the circular solution should be adopted. Because of this result and the possible bias introduced by the very unequal phase distribution of the McDonald Observatory velocities, we have chosen to adopt a circular orbit solution for 108 Her.

The velocities of Ludendorff (1914) and Daniel & Jenkins (1916) are not precise enough to improve our orbital solution. To see whether the velocities of Abt & Levy (1985) warrant inclusion in our combined orbital solution, we reexamined the orbit of Abt & Levy (1985), using their primary velocities alone. Adopting their period, which is substantially different from the one computed by Daniel & Jenkins (1916) as well as the one determined in this paper, produces an extremely poor fit to their data. Reanalysis of their primary velocities with the period as a free parameter results in a period that is similar in value to

Table 6
Radial Velocities of 108 Her

Hel. Julian Date (HJD − 2,400,000)	Phase	V_1 (km s^{-1})	$(O-C)_1$ (km s^{-1})	Wt_1	V_2 (km s^{-1})	$(O-C)_2$ (km s^{-1})	Wt_2	Source[a]
52,391.888	0.116	31.1	−0.2	1.0	−89.8	−0.2	0.3	McD
52,392.877	0.296	−45.4	−0.2	1.0	1.0	0.4	0.3	McD
52,393.912	0.483	−98.1	0.1	1.0	63.4	0.3	0.3	McD
52,749.915	0.040	48.0	0.0	1.0	−108.7	0.6	0.3	McD
52,750.921	0.222	−11.2	−0.1	1.0	−39.9	−0.4	0.3	McD
52,888.709	0.208	−4.9	−0.2	1.0	−47.2	−0.1	0.3	McD
52,889.638	0.376	−77.2	0.1	1.0	38.5	0.0	0.3	McD
52,889.778	0.402	−84.8	0.1	1.0	47.4	0.0	0.3	McD
52,890.634	0.557	−93.9	0.0	1.0	58.2	0.2	0.3	McD
53,108.966	0.149	20.1	0.0	1.0	−76.3	0.1	0.3	McD
53,110.934	0.505	−98.7	−0.1	1.0	63.7	0.1	0.3	McD
53,119.970	0.144	21.7	−0.1	0.4	−78.2	0.2	0.1	KPNO
53,121.979	0.508	−98.4	0.1	0.4	64.0	0.5	0.1	KPNO
53,123.949	0.866	25.4	0.1	0.4	−82.3	0.2	0.1	KPNO
53,168.819	0.002	50.2	−0.1	0.4	−112.1	−0.1	0.1	KPNO
53,172.738	0.713	−41.6	−0.2	0.4	−4.5	−0.7	0.1	KPNO
53,173.809	0.907	37.9	0.0	0.4	−97.8	−0.4	0.1	KPNO
53,260.655	0.655	−66.3	−0.4	1.0	25.2	0.2	0.3	McD
53,260.740	0.671	−59.9	−0.2	1.0	17.9	0.1	0.3	McD
53,261.667	0.839	15.2	−0.1	1.0	−70.3	0.4	0.3	McD
53,491.017	0.428	−91.4	−0.2	0.4	54.8	−0.1	0.1	KPNO
53,491.961	0.600	−84.6	0.0	0.4	47.1	0.1	0.1	KPNO
53,533.806	0.188	4.7	0.4	0.4	−58.2	−0.5	0.1	KPNO
53,534.732	0.355	−70.1	−0.1	0.4	29.5	−0.3	0.1	KPNO
53,851.934	0.876	28.5	−0.2	0.4	−86.8	−0.3	0.1	KPNO
53,852.933	0.057	45.7	0.1	0.4	−106.0	0.4	0.1	KPNO
53,912.936	0.938	44.9	0.2	0.4	−105.8	−0.5	0.1	KPNO
53,915.891	0.473	−97.6	0.0	0.4	63.0	0.6	0.1	KPNO
54,001.617	0.019	49.9	0.1	0.4	−110.5	0.9	0.1	KPNO
54,002.684	0.212	−6.7	0.0	0.4	−43.8	1.0	0.1	KPNO
54,006.660	0.933	44.1	0.3	0.4	−104.0	0.3	0.1	KPNO
54,221.913	0.966	48.5	−0.1	0.4	−110.0	0.0	0.1	KPNO
54,222.910	0.147	20.7	0.0	0.4	−77.2	−0.2	0.1	KPNO
54,266.822	0.110	33.1	−0.1	0.4	−91.7	0.1	0.1	KPNO
54,268.848	0.477	−97.5	0.4	0.4	62.3	−0.4	0.1	KPNO
54,583.946	0.616	−79.9	−0.2	0.4	41.0	−0.3	0.1	KPNO
54,585.015	0.810	3.9	0.7	0.4	−56.4	0.1	0.1	KPNO
54,643.849	0.479	−97.9	0.1	0.4	62.5	−0.3	0.1	KPNO
54,731.621	0.395	−83.1	−0.1	0.4	45.2	0.0	0.1	KPNO
54,732.632	0.578	−89.9	−0.1	0.4	53.2	0.0	0.1	KPNO

Note. [a] McD: McDonald Observatory, KPNO: Kitt Peak National Observatory.

ours. Thus, perhaps the period given by Abt & Levy (1985) is a transcription error.

We computed individual orbital solutions to determine the weights for each set of velocities. For the primary those weights are 1.0, 0.4, and 0.004 for the McDonald, KPNO, and Abt & Levy (1985) KPNO velocities, respectively. A combined solution with those three data sets, compared to a solution with just our McDonald and KPNO velocities, resulted in a slightly more precise period because of the longer time span of the data. However, the periods that were determined in the two solutions differ by less than their 1σ uncertainties, and the uncertainties of the other elements were not improved with the addition of the Abt & Levy (1985) velocities. Thus, we have chosen not to include any of the Abt & Levy (1985) velocities in our later solutions. We next determined weights for the secondary component, which are 0.3 and 0.1 for our McDonald and KPNO velocities, respectively. With our McDonald and KPNO velocities for both stars appropriately weighted, we computed a final combined circular orbit solution (Table 7). The 14 McDonald Observatory and 26 KPNO observations used for this orbital solution are given in Table 6.

Table 7 lists the resulting elements for our final orbit, as well as the orbital elements of Abt & Levy (1985). The much smaller uncertainties of our elements are obvious. The problem with the period derived by Abt & Levy (1985) has been discussed above. In addition, although our mass ratio is very similar to theirs, our minimum masses are more than 20% larger. Finally, Figure 3 compares our new primary and secondary velocities with the calculated velocity curves. Zero phase for that orbit is a time of maximum velocity for the primary.

5. SPECTRAL TYPES AND MAGNITUDE DIFFERENCE

Strassmeier & Fekel (1990) identified several luminosity-sensitive and temperature-sensitive line ratios in the 6430–6465 Å region. They employed those critical line ratios and the general appearance of the spectrum as spectral-type criteria. However, for stars that are hotter than early-G spectral class,

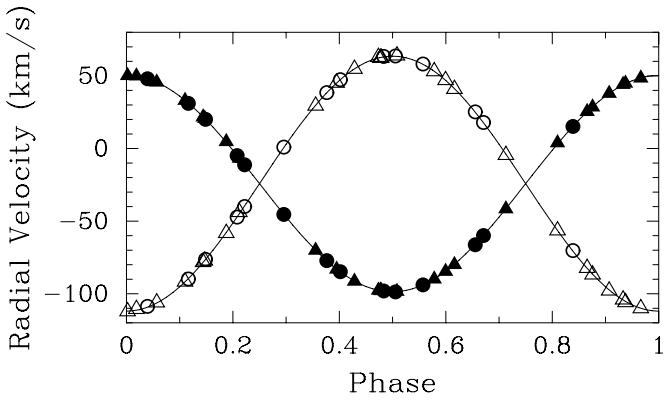

Figure 3. Radial velocities of 108 Her compared with the computed velocity curves. The filled and open symbols represent the primary and secondary, respectively. Circles: McDonald Observatory; triangles: KPNO. Zero phase is a time of maximum velocity of the primary.

Table 7
Orbital Elements and Related Properties of 108 Her

Parameter	Abt & Levy (1985)	This Study
P (days)	5.51274 ± 0.00005	5.5146126 ± 0.0000041
T_0 (HJD)	2,440,001.080 ± 0.029	2,453.124.6904 ± 0.0004
e	0.001 ± 0.025	0.0 (adopted)
ω (deg)	...	...
K_1 (km s^{-1})	70.1 ± 1.2	74.477 ± 0.039
K_2 (km s^{-1})	81.9 ± 2.1	87.788 ± 0.075
γ (km s^{-1})	−21.9 ± 1.2	−24.175 ± 0.026
$m_1 \sin^3 i$ ($M_\odot$)	1.08	1.3238 ± 0.0024
$m_2 \sin^3 i$ ($M_\odot$)	0.93	1.1230 ± 0.0015
$a_1 \sin i$ (10^6 km)	5.314	5.6477 ± 0.0030
$a_2 \sin i$ (10^6 km)	6.208	6.6571 ± 0.0057
rms residual (km s^{-1}) (unit weight)	...	0.14

the line ratios in that wavelength region have little sensitivity to luminosity. Thus, for the A and F stars of our three systems, we have used the entire 84 Å spectral region of our KPNO observations to estimate just the spectral classes of the individual components. The luminosity class may be determined by computing the absolute visual magnitude with the *Hipparcos* parallax and comparing that magnitude to evolutionary tracks or a table of canonical values for giants and dwarfs.

Spectra of our three binaries were compared with the spectra of a number of A, F, and early-G-type stars primarily from the lists of Abt & Morrell (1995) and Fekel (1997). The reference-star spectra were obtained at KPNO with the same telescope, spectrograph, and detector as our binary-star spectra. To facilitate a comparison, various combinations of the reference-star spectra were rotationally broadened, shifted in radial velocity, appropriately weighted, and added together with a computer program developed by Huenemoerder & Barden (1984) and Barden (1985) in an attempt to reproduce the binary spectra.

That analysis has met with limited success for two of our three star systems, HD 82191 and 108 Her, because those binaries contain Am stars. Classical Am stars have spectral classes of A4–F1, determined from their hydrogen lines (Abt & Morrell 1995). Such stars are noted as having peculiar spectra because lines of their metallic elements such as iron and strontium are stronger than expected compared to the hydrogen classification, while elements such as calcium and scandium are weaker (Abt & Morrell 1995). There are no hydrogen lines

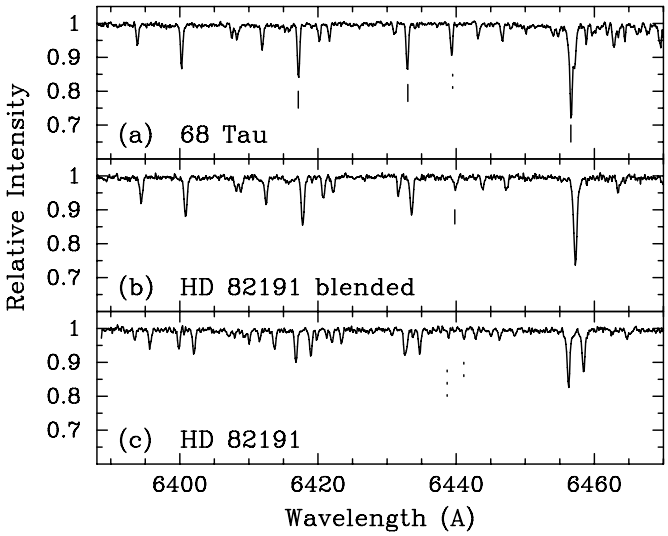

Figure 4. (*a*) Spectrum of 68 Tau in the 6430Å region. The three strongest Fe II lines are indicated with solid lines, the strongest Ca I line is identified with a dashed line. (*b*) Spectrum of HD 82191 at a blended phase. The dashed line identifies the same Ca I line as in (*a*), and that feature is clearly significantly weaker in HD 82191 than in 68 Tau. (*c*) Spectrum of HD 82191 at a double-lined phase. The same Ca I line in both components is identified. The longer dashed line indicates the primary.

in our limited 6430 Å wavelength region, and the iron and calcium abundance peculiarities vary from star to star, making it impossible to completely characterize the composite spectra of the two binaries by combining our limited number of reference spectra.

For the third system, ω Dra, we have been able to determine a best spectrum model, which has been used to determine the continuum intensity ratio of the binary components at 6430 Å, a wavelength that is about 0.6 of the way between the central wavelengths of the Johnson V and R bandpasses. If the two stars have very similar spectral types, this intensity ratio is also the luminosity ratio and, thus, can be converted directly into a magnitude difference. However, if the lines of the secondary are intrinsically stronger than those of the primary, as is the case for ω Dra, which has main-sequence stars of rather different spectral types, then the continuum intensity ratio results in a minimum magnitude difference.

5.1. HD 82191

Gulliver (1971) identified HD 82191 as an Am star, and Heard & Hurkens (1973) judged the system to have A1, mid A, and F0 spectral classes for its calcium, hydrogen, and metal lines, respectively. Such a classification is quite different from that of Abt (2004), who classified the combined spectrum as A0 Vs.

Figure 4 compares a spectrum of 68 Tau (panel (a)) to a blended spectrum (panel (b)) and a double-lined spectrum (panel (c)) of HD 82191. Although Cowley et al. (1969) and Abt & Morrell (1995) classified 68 Tau as A2 IV, Conti (1965) identified it as one of the prototypes for the extension of Am stars to early-A spectral types. Conti (1965) also discussed why visual identification of Am star anomalies is difficult for these hotter A stars. In the case of 68 Tau its Am nature has been confirmed by several abundance analyses, including those of Varenne & Monier (1999) and Pintado & Adelman (2003).

The most numerous lines of 68 Tau in the 6430 Å region are Fe I lines. However, because of its effective temperature, the three strongest features of 68 Tau in this wavelength region are

Fe II lines, which are indicated, along with the strongest Ca I line, in Figure 4. Most of the lines in the spectrum of 68 Tau that are redward of the Fe II line at 6457 Å are terrestrial water vapor lines. Ignoring those lines, the blended spectrum of HD 82191 (panel (b)) appears similar to that of 68 Tau except for the calcium line at about 6440 Å, which is significantly weaker in HD 82191. The spectrum of HD 82191 in panel (c), which shows lines of the individual components, enables us to identify the star with the stronger Fe II lines and the weaker Fe I lines as the more massive primary. From spectrum addition fits with 68 Tau to the individual components of HD 82191 we estimate that the spectral classes for the iron lines of the primary and secondary are about A1 and A4, respectively. Relative to 68 Tau, previously identified as an Am star, the primary is clearly deficient in calcium, and the secondary probably is as well. Thus, we concur with the conclusion of Heard & Hurkens (1973) that both components are Am stars.

From the ratio of the line depths of the Fe II lines the magnitude difference between the components is 0.2 mag at 6430 Å, essentially the same as that found by Heard & Hurkens (1973) from their blue spectrograms. Even adopting a larger magnitude difference, as discussed in Section 6.1, the *Hipparcos* parallax (Perryman et al. 1997) indicates that both stars are on the main sequence.

5.2. ω Dra

Both Roman (1950) and Slettebak (1955) classified the combined spectrum of ω Dra as F5 V, similar to the more recent spectral type of F4 V given by Cowley (1976). The reference stars θ Cyg (F4 V (Slettebak 1955) and mean [Fe/H] = 0.01 (Taylor 2005)) and λ Ser (G0 V (Keenan & McNeil 1989) and mean [Fe/H] = 0.00 (Taylor 2005)) produce an excellent fit to the components.

The continuum intensity ratio of the secondary/primary is 0.376, which results in a continuum magnitude difference of 1.06 at 6430 Å. The secondary has a significantly later spectral class than the primary, and so this is a minimum value. As discussed in Section 6.2, the *Hipparcos* parallax (Perryman et al. 1997) indicates that both stars are on the main sequence.

5.3. 108 Her

Classifiers have identified 108 Her as an Am star, with Abt & Morrell (1995) concluding that the combined spectrum has types A3/F0/F0 for the Ca I K line, the Balmer lines, and the metals. From our visual examination of the 6430 Å region, it is clear that the primary is an Am star. Although we are unable to find an Am reference star among our collection of spectra that reasonably approximates the primary's spectrum, comparing the ratio of the Fe II and Fe I lines to those of several reference stars, we estimate that the spectral class of the iron lines is A7. The calcium lines of the primary are weak and thus, have an earlier spectral class, which we estimate as A3. The iron and calcium lines of the secondary in the 6430 Å region are well matched by the A9 V spectrum (Abt & Morrell 1995) of HR 1613, which has normal rather than peculiar abundances of those elements (Bikmaev et al. 2002). Thus, we conclude that the primary is an Am star, while the secondary has a spectral class of A9.

Comparing several Fe I lines, the average ratio of their equivalent widths is 0.57, which translates to a magnitude difference of 0.6 at 6430 Å. This is a lower limit to that difference because the Am star's iron line strengths are somewhat enhanced. With such a magnitude difference or even significantly larger ones (Section 6.3), the *Hipparcos* parallax (Perryman et al. 1997) indicates that both stars are on the main sequence.

6. CIRCULARIZATION AND SYNCHRONIZATION

According to the two main theories of orbital circularization and rotational synchronization (e.g., Zahn 1977; Tassoul & Tassoul 1992), synchronization should occur first. Observationally, Matthews & Mathieu (1992) examined a sample of 62 spectroscopic binaries with A-type primaries and periods less than 100 days. They concluded that all systems with orbital periods $\lesssim 3$ days have circular or nearly circular orbits and found that many binaries with periods in the range of 3–10 days also have circular orbits. Duquennoy & Mayor (1991) investigated the multiplicity of solar-type stars in the solar neighborhood. They determined that while systems with periods $\leqslant 10$ days had circular orbits, longer period orbits are generally eccentric. Although two of our systems have A-type primaries, all three binary periods are less than 10 days, so it is not particularly surprising that our three systems have circular orbits.

To help in assessing synchronization, we have determined projected rotational velocities from our red-wavelength KPNO spectra with the procedure of Fekel (1997), measuring the line broadening, removing the instrumental broadening, and using an empirical calibration polynomial (Fekel 1997) to convert the broadening in angstroms into units of kilometers per second. For A-type stars this line broadening corresponds to the v sin i value. For F- and G-type stars, macroturbulent broadening has been taken into account. Following Fekel (1997), for mid-F and early-G stars values of 4 and 3 km s^{-1}, respectively, were used. To convert the v sin i values into equatorial rotational velocities, we assume, as is generally done, that the axes of the orbital and rotational planes are parallel, so the inclinations are equal.

6.1. HD 82191

To determine if the components of HD 82191 are synchronously rotating, we must first estimate their radii. Although the system is believed to be eclipsing, no light-curve solution is available. Thus, we obtain its radii using the Stefan–Boltzmann law. From the *Hipparcos* catalog (Perryman et al. 1997) the V magnitude and $B-V$ color of the HD 82191 system are 6.64 and 0.08, respectively. The *Hipparcos* parallax of 7.11 ± 0.84 mas (Perryman et al. 1997) corresponds to a distance of 141 ± 17 pc. Although at such a distance there may be a slight amount of interstellar reddening, we have assumed that there is none.

While our magnitude difference from Section 5.1 indicates that the stars are nearly equal in brightness, the primary to secondary mass ratio of 1.2 suggests otherwise. Thus, we have adopted the 0.8 mag difference from the mass–luminosity calibration of Smith (1983), which increases the apparent magnitude of the primary by 0.4 mag. The parallax, the V magnitude, and the adopted V magnitude difference were combined to obtain absolute magnitudes $M_V = 1.3 \pm 0.3$ mag and $M_V = 2.1 \pm 0.3$ mag for the primary and secondary, respectively. We next adopted $B - V$ colors of 0.06 and 0.12 for the primary and secondary, respectively, and then used Table 3 of Flower (1996) to obtain the bolometric corrections and effective temperatures of the two components. The resulting luminosities of the primary and secondary are $L_1 = 24.8 \pm 7.4\ L_\odot$ and $L_2 = 11.3 \pm 3.4\ L_\odot$, respectively, while the radii are $R_1 = 2.1 \pm 0.4\ R_\odot$ and $R_2 = 1.6 \pm 0.3\ R_\odot$, respectively. The uncertainties in the computed quantities are primarily due to the parallax

uncertainty plus, to a lesser extent, the effective temperature uncertainty, which is estimated to be ± 300 K.

For HD 82191 our v sin i values, averaged from eight spectra, are 11.7 ± 1.0 and 11.9 ± 1.0 km s^{-1} for the primary and secondary, respectively. The minimum masses of the two components are relatively large, and Fernie (1974) detected a partial eclipse of the primary, indicating that the orbital inclination is not too far from 90°. Choosing a somewhat smaller inclination of 85° does not significantly increase our projected rotational velocities, and so we adopt 12 km s^{-1} as the equatorial rotational velocity for both components. The estimated radii result in rotational velocities of 11.8 and 9.0 km s^{-1} for the primary and secondary, respectively. Thus, the primary is synchronously rotating, while the secondary appears to be rotating faster than synchronous. However, given the uncertainty of the secondary's estimated radius, and the difficulty in measuring the broadening of the very weak lines of the secondary, it is possible that the secondary is also synchronously rotating.

6.2. ω Dra

Similar to HD 82191, the answer to the question of whether the components of ω Dra are synchronously rotating begins with estimates of the components' radii. From the *Hipparcos* catalog (Perryman et al. 1997) the V magnitude and $B-V$ color of the ω Dra system are 4.77 and 0.43, respectively. The *Hipparcos* parallax of 42.62 ± 0.53 mas (Perryman et al. 1997) corresponds to a distance of 23.46 ± 0.29 pc. From a consideration of our spectral types and minimum magnitude difference, we adopted a V magnitude difference of 1.2, slightly larger than the canonical value given by Gray (1992). The parallax, the V magnitude, and the adopted V magnitude difference were combined to obtain absolute magnitudes M_V = 3.2 ± 0.1 mag and M_V = 4.4 ± 0.2 mag for the primary and secondary, respectively. We next assumed $B-V$ colors of 0.40 and 0.58 (Gray 1992), for the primary and secondary, respectively, and then used Table 3 of Flower (1996) to obtain the bolometric corrections and effective temperatures of the two components. The resulting luminosities of the primary and secondary are $L_1 = 4.0 \pm 0.4\ L_\odot$ and $L_2 = 1.4 \pm 0.3\ L_\odot$, respectively, while the radii are $R_1 = 1.5 \pm 0.1\ R_\odot$ and $R_2 = 1.1 \pm 0.1\ R_\odot$, respectively. These values indicate that both components are on the main sequence. The uncertainties in the computed quantities are dominated by the parallax and the effective temperature uncertainties. The latter is estimated to be ±200 K for the primary and ± 150 K for the secondary.

For ω Dra our v sin i values, averaged from eighteen KPNO spectra, are 7.2 ± 1.0 and 7.1 ± 2.0 km s^{-1} for the primary and secondary, respectively. The estimated uncertainty for the secondary is larger because the lines of the secondary are significantly weaker than those of the primary and thus, are more susceptible to blends that would increase the line broadening. The minimum masses of the components are very small, and so we adopt the canonical masses (Gray 1992) for our spectral types, which produce an orbital inclination of 29°. Assuming this value for the rotational inclination increases the rotational velocities to 14 km s^{-1} for both components. Our computed radii result in velocities of 14 and 10.5 km s^{-1}. Taken at face value, the primary is synchronously rotating, while the secondary is not. However, the errors for the various values produce a near overlap of the predicted and observed rotational velocities, so we do not completely rule out the possibility that the secondary is also rotating synchronously.

6.3. 108 Her

To see if the components of 108 Her are synchronously rotating, we once again begin by determining the radii of the components. Our spectral type for the secondary corresponds to a mass of 1.6 $M_\odot$ (Gray 1992). That value and the primary to secondary mass ratio of 1.18 result in a mass of 1.9 $M_\odot$ for the primary. With those masses and the mass–luminosity calibration of Smith (1983), we obtained a magnitude difference of 0.7, which increases the apparent magnitude of the primary by 0.46 mag. The parallax, the V magnitude, and the adopted V magnitude difference were combined to obtain absolute magnitudes M_V = 2.3 ± 0.3 mag and M_V = 3.0 ± 0.3 mag for the primary and secondary, respectively. We next assumed $B-V$ colors of 0.14 and 0.26 for the primary and secondary, respectively, and then used Table 3 of Flower (1996) to obtain the bolometric corrections and effective temperatures of the two components. The resulting luminosities of the primary and secondary are $L_1 = 9.6 \pm 2.7\ L_\odot$ and $L_2 = 5.0 \pm 1.4\ L_\odot$, respectively, while the radii are $R_1 = 1.6 \pm 0.3\ R_\odot$ and $R_2 = 1.4 \pm 0.2\ R_\odot$, respectively. As is generally the case, uncertainties in our computed quantities are dominated by the parallax uncertainty. Additional uncertainty results primarily from the effective temperature uncertainty, which is estimated to be ± 300 K. These radii appear to be about 0.2 $R_\odot$ smaller than expected canonical values for main-sequence stars of A spectral type (e.g., Gray 1992), but the uncertainties are large enough to produce an overlap of the values.

For 108 Her our v sin i values, averaged from 20 spectra, are 14.3 ± 1.0 and 12.8 ± 1.0 km s^{-1} for the primary and secondary, respectively. Our adopted masses result in an inclination of 69° and so increase the rotational velocities to 15 and 14 km s^{-1}. Our computed radii result in synchronous velocities of 15 and 13 km s^{-1} for the primary and secondary, respectively, so it appears that both components are synchronously rotating.

7. CONCLUSIONS

We have determined new, precise, circular spectroscopic orbits for the bright double-lined spectroscopic binaries HD 82191, ω Dra, and 108 Her. While our improved minimum masses are in reasonable accord with the best earlier determinations for HD 82191 and ω Dra, our values for 108 Her are more than 20% larger than previously calculated. The adopted orbital inclinations result in masses for the various components. Those values and the respective *Hipparcos* parallaxes of the systems, combined with Kepler's third law, produce angular semimajor axes of the orbits, which are 0.93 mas for HD 82191, 3.4 mas for ω Dra, and 1.6 mas for 108 Her. Doubling those values results in maximum angular separations ranging from 2 to 7 mas for the binary components, enabling the systems to be resolved with modern optical interferometers. High-precision interferometric observations, combined with our spectroscopic results, will produce accurate three-dimensional orbits, masses, and distances for the systems. We conclude that both components of HD 82191 are Am stars as is the primary of 108 Her. However, its A9 secondary has normal abundances. We estimate spectral types of F4 dwarf and G0 dwarf for the components of ω Dra. All six components of the three binary systems are either definitely or possibly synchronously rotating.

We thank David Doss for his patient guidance, which was essential for the successful operation of the 2.1 m telescope at McDonald and its instrumentation, and Daryl Willmarth for his

support of the KPNO coudé feed observations. The research at Tennessee State University was supported in part by NASA grant NCC5-511 and NSF grant HRD-9706268.

REFERENCES

Abt, H. A. 1975, ApJ, 195, 405
Abt, H. A. 2004, ApJS, 155, 175
Abt, H. A., & Bidelman, W. 1969, ApJ, 158, 1091
Abt, H. A., & Levy, S. G. 1976, ApJS, 30, 273
Abt, H. A., & Levy, S. G. 1985, ApJS, 59, 229
Abt, H. A., & Morrell, N. I. 1995, ApJS, 99, 135
Adams, W. S. 1912, ApJ, 35, 163
Barden, S. C. 1985, ApJ, 295, 162
Barker, E. S., Evans, D. S., & Laing, J. D. 1967, R. Obs. Bull., 130, 355
Batten, A. H., Fletcher, J. M., & MacCarthy, D. G. 1989, Publ. Dom. Astrophys. Obs., 17, 1
Bertaud, C. 1970, A&AS, 1, 7
Bikmaev, I. F., et al. 2002, A&A, 389, 537
Boden, A. F., Torres, G., & Latham, D. W. 2006, ApJ, 644, 1193
Burkhart, C., & Coupry, M. F. 1991, A&A, 249, 205
Campbell, W. W. 1899, ApJ, 10, 178
Conti, P. S. 1965, ApJ, 142, 1594
Cowley, A. 1976, PASP, 88, 95
Cowley, A., Cowley, C., Jaschek, M., & Jaschek, C. 1969, AJ, 74, 375
Daniel, Z., & Jenkins, L. F. 1916, Publ. Allegheny Obs., 3, 147
Duquennoy, A., & Mayor, M. 1991, A&A, 248, 485
Eaton, J. A., & Williamson, M. H. 2004, Proc. SPIE, 5496, 710
Eaton, J. A., & Williamson, M. H. 2007, PASP, 119, 886
Favata, F., Barbera, M., Micela, G., & Sciortino, S. 1995, A&A, 295, 147
Fekel, F. C. 1997, PASP, 109, 514
Fernie, J. D. 1974, Info. Bull. Var. Stars, 872, 1
Flower, P. J. 1996, ApJ, 469, 355
Gray, D. F. 1992, The Observation and Analysis of Stellar Photospheres (Cambridge: Cambridge Univ. Press)
Gulliver, A. F. 1971, M.Sc. thesis Univ. of Toronto
Heard, J. F., & Hurkens, R. 1973, J. R. Astron. Soc. Canada, 67, 306
Herbig, G. H., & Spalding, J. F., Jr. 1955, ApJ, 121, 118
Huenemoerder, D. P., & Barden, S. C. 1984, BAAS, 16, 510
Hummel, C. A., et al. 2001, AJ, 121, 1623
Keenan, P. C., & McNeil, R. C. 1989, ApJS, 71, 245
Levato, H. 1975, A&AS., 19, 91
Lucy, L. B., & Sweeney, M. A. 1971, AJ, 76, 544
Luddendorff, H. 1914, Astron. Nach., 197, 217
Luyten, W. J. 1936, ApJ, 84, 85
Matthews, L. D., & Mathieu, R. D. 1992, in ASP Conf. Ser. 32, Complimentary Approaches to Double and Multiple Star Research, IAU Colloquium 135, ed. H. A. Hartkopf & W. I. McAlister (San Francisco, CA: ASP), 244
Mayor, M., & Mazeh, T. 1987, A&A, 171, 157
McCarthy, J. A., Sandiford, B. A., Boyd, D., & Booth, J. 1993, PASP, 105, 881
Moore, C. E., Minnaert, M. G. J., & Houtgast, J. 1966, The Solar Spectrum 2935 Å to 8770 Å, National Bureau of Standards Monograph 61 (Washington, DC: U. S. Government Printing Office)
Perryman, M. A. C., et al. 1997, A&A, 323, L49
Pintado, O. I., & Adelman, S. J. 2003, A&A, 406, 987
Pourbaix, D., et al. 2004, A&A, 424, 727
Quirrenbach, A. 2001, Ann. Rev. Astron. Astrophys., 39, 353
Roman, N. G. 1950, ApJ, 112, 554
Scarfe, C. D., Batten, A. H., & Fletcher, J. M. 1990, Publ. Dom. Astrophys. Obs., 18, 21
Slettebak, A. 1955, ApJ, 121, 653
Smith, R. C. 1983, The Observatory, 103, 29
Stickland, D. J. 1973, MNRAS, 161, 193
Strassmeier, K. G., & Fekel, F. C. 1990, A&A, 230, 389
Tassoul, J.-L., & Tassoul, M. 1992, ApJ, 395, 259
Taylor, B. J. 2005, ApJS, 161, 444
Tomkin, J., & Fekel, F. C. 2006, AJ, 131, 2652
Tomkin, J., & Fekel, F. C. 2008, AJ, 135, 555
Turner, A. B. 1907, ApJ, 26, 277
Varenne, O., & Monier, R. 1999, A&A, 351, 247
Wolfe, R. H., Horak, H. G., & Storer, N. W. 1967, in Modern Astrophysics, ed. M. Hack (New York: Gordon & Breach), 251
Young, R. K. 1942, Publ. David Dunlap Obs., 1, 251
Zahn, J.-P. 1977, A&A, 57, 383